Electronic Supplementary Material (ESI) for Materials Advances.

Reductive processing of single walled carbon nanotubes for high volumetric performance supercapacitors

Pichamon Sirisinudomkit,[a,b] Evgeny Senokos, [b] Noelia Rubio,[b] and Milo S. P. Shaffer [*a,b]

a) Department of Materials, Imperial College London, SW7 2AZ, UK

b) Department of Chemistry, Imperial College London, SW7 2AZ, UK

*Corresponding author E-mail address: m.shaffer@imperial.ac.uk

1. Calculation

The specific capacitance of the electrode in 3-electrode system

The gravimetric ($C_{s,CV}$) and volumetric ($C_{v,CV}$) capacitance of the electrode can be determined from the Cyclic voltammetry (CV) technique by the following equations S1 and S2;

$$C_{s,cv} = \frac{\int idv}{\Delta V_{cv} \times m \times v} \quad \text{(S1)}$$

$$C_{v,cv} = \rho C_{s,cv} \quad \text{(S2)}$$

where $\int idv$ is an integral under CV discharge curve, ΔV_{cv} is a working potential window (V) and m is a total mass of the electrode. v is the scan rate and ρ is the density of the electrode.

The gravimetric ($C_{s,GCD}$) and volumetric ($C_{v,GCD}$) capacitances of the electrode can also be determined from the galvanostatic charge discharge (GCD) technique by the following equations S3 and S4;

$$C_{s,GCD} = \frac{I_{GCD}}{m \times (\frac{dV}{dt})} \quad \text{(S3)}$$

$$C_{v,GCD} = \rho C_{s,GCD} \quad \text{(S4)}$$

where I_{GCD} is the applied constant current (A), $\frac{dV}{dt}$ is calculated from the slope obtained by fitting the discharge curve.

The specific capacitance of as-fabricated device

The specific capacitance of the as-fabricated device was evaluated according to equations S5 and S6

$$C_{cell,s} = \frac{I_{GCD}}{m_d \times (\frac{dV}{dt})} \quad \text{(S5)}$$

$$C_{cell,v} = \frac{I_{GCD}}{V_d \times (\frac{dV}{dt})} \quad \text{(S6)}$$

where m_d and V_d are the total mass and volume of full device, including the mass and volume of active materials, separator and electrolyte.

The electrolyte mass

The electrolyte mass (m_e) was calculated via the equation below:

$$m_e = \rho_e(2f_w(V_w) + f_s(V_s)) \quad \text{(S7)}$$

where ρ_e is the density of the electrolyte, f_w is the porosity and V_w is total volume of active electrode. f_s is the porosity and V_s is total volume of separator.

In order to compare the capacitance of the device with 3-electrode system and other CNT-based supercapacitors in the literature, the specific capacitance was calculated via

$$C_{cell,s} = 4\frac{I_{GCD}}{m \times \left(\frac{dV}{dt}\right)} \quad \text{(S8)}$$

where m is total mass of electrode materials

Specific energy and specific power of the supercapacitor devices

Specific energy (E_{cell}) and specific power (P_{cell}) were calculated by integrating discharge curves of full devices as follows:

$$E_{cell} = i\int Vdt \quad \text{(S9)}$$

$$P_{cell} = \frac{E_{cell}}{t_{discharge}} \quad \text{(S10)}$$

where i is the constant applied current density, $\int Vdt$ is the integrating area under discharge curve and $t_{discharge}$ is the discharging time.

The Coulombic efficiency

The Coulombic efficiency(η) was calculated from the ratio of discharging time and charging time at the same current density by the following equation (S11):

$$\eta = (\frac{t_{discharge}}{t_{charge}}) \times 100\% \quad \text{(S11)}$$

where $t_{discharge}$ is the discharging time and t_{charge} is charging time.

2. The optimisation of charge functionalisation

2.1. C:Na control at 10:1 (molar ratio)

Nanotubide buckypapers in this section were prepared from the bulk nanotubide solution at a stoichiometry of 10 C:1 Na then, diluting the solution to 1-4 mg/ml with DMAc. Each piece of buckypaper contains 7 mg of SWCNTs.

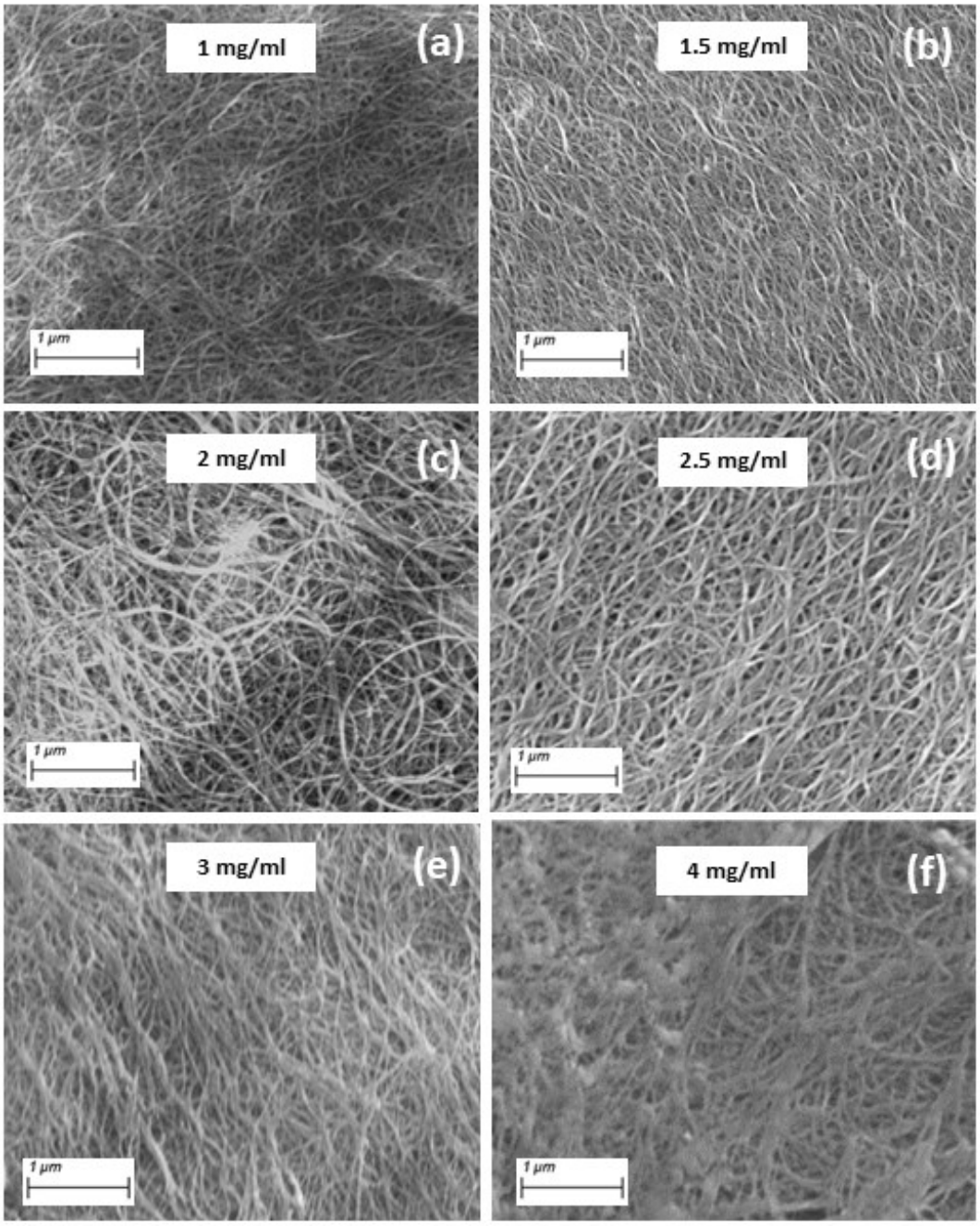

Fig.S1 SEM images of nanotubide buckypapers with different **[C]** concentration (holding C:Na ratio constant at 10:1) **(**a**)** 1 mg**/**ml, **(**b**)** 1**.**5 mg**/**ml, **(**c**)** 2 mg**/**ml, **(**d**)** 2**.**5 mg**/**ml, **(**e**)** 3 mg**/**ml and **(**f**)** 4 mg**/**ml**.**

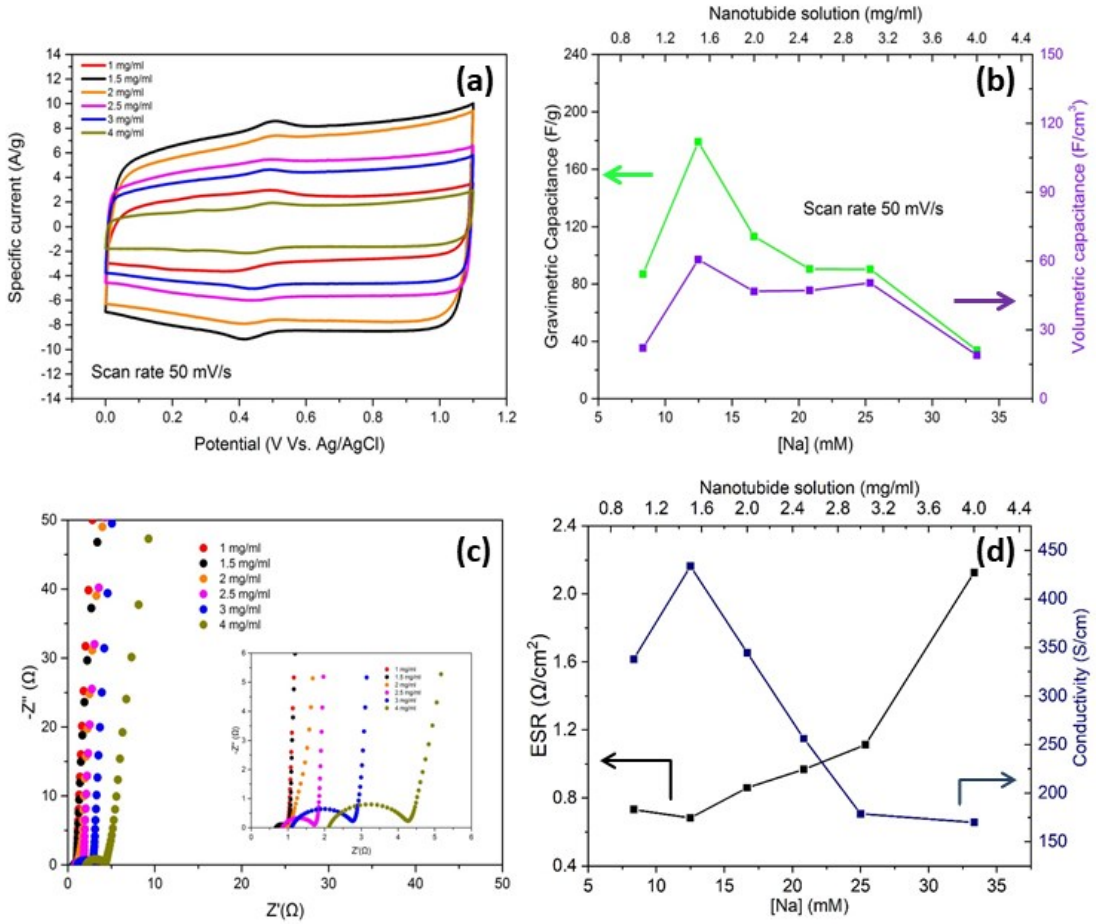

Fig.S2 (a) CV curves at 50 mV/s and (b) gravimetric and volumetric capacitance vs. sodium concentration of nanotubide buckypapers at different carbon concentration. (c) Nyquist plots and (d) ESR and conductivity of nanotubide buckypapers at different absolute carbon concentration (holding C:Na ratio constant at 10:1) in 1M H_2SO_4.

2.2. SWCNTs/DMAc concentration ([C]) control at 1.5 mg/ml

Nanotubide buckypapers in this section were prepared from nanotubide solution at C:Na stoichiometry varied from 5:1 to 15:1. The concentration of SWCNTs in DMAc was controlled at 1.5 mg of SWCNTs/ 1 ml of DMAc. Each piece of buckypaper contains 7 mg of SWCNTs. For XPS data, the O1s spectra of nanotubide buckypaper ([C] = 1.5 mg/ml, C:Na=10:1) shows three peaks at 533.4, 532.4 and 531.5 eV which are assigned to C-OH, C=O and -COOH functional groups, respectively.[1, 2]

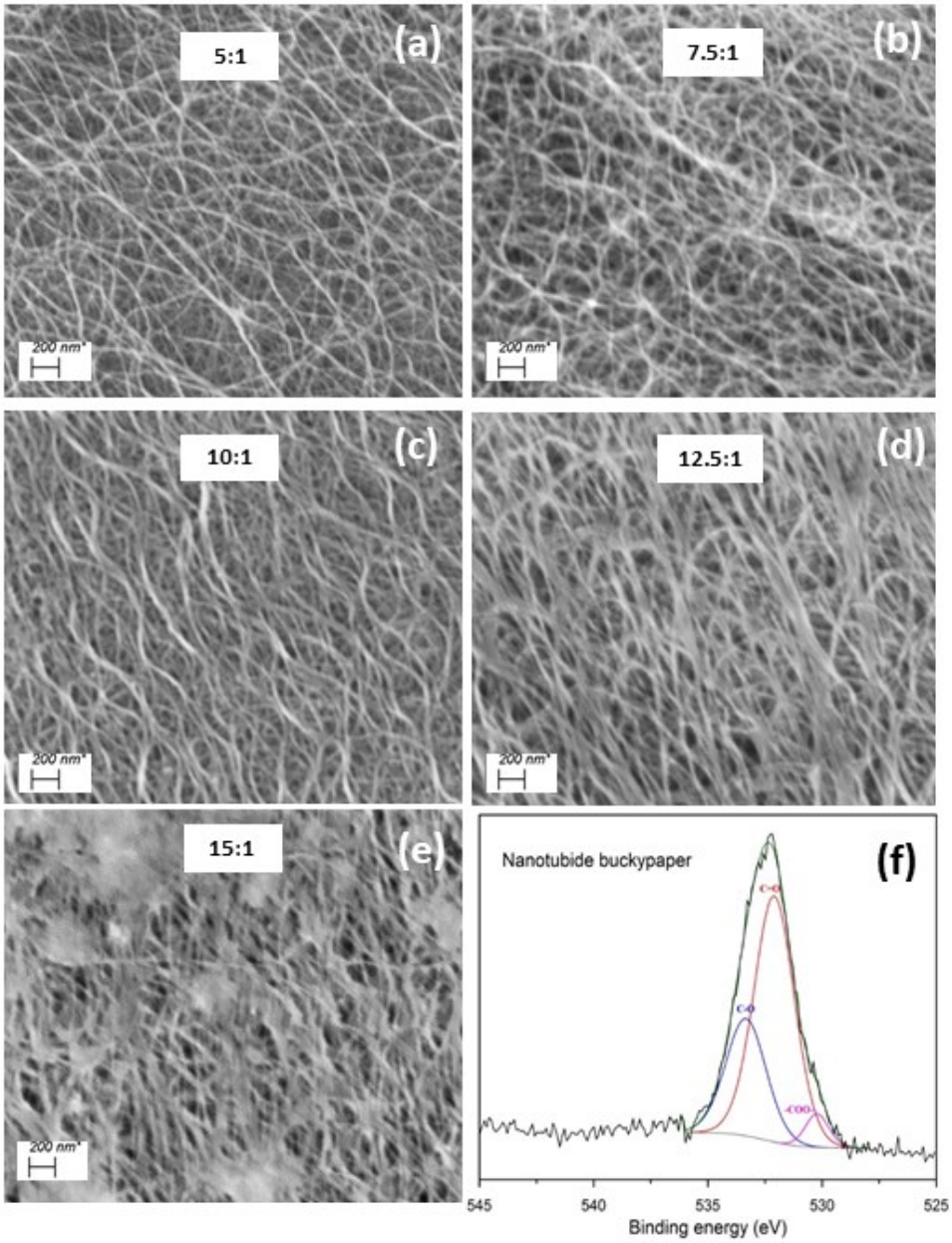

Fig.S3 (a-e**)** SEM images of nanotubide buckypapers at different C:Na and **(**f**)** O1s of optimised nanotubide buckypaper ([C] = 1.5 mg/ml, C:Na=10:1)**.**

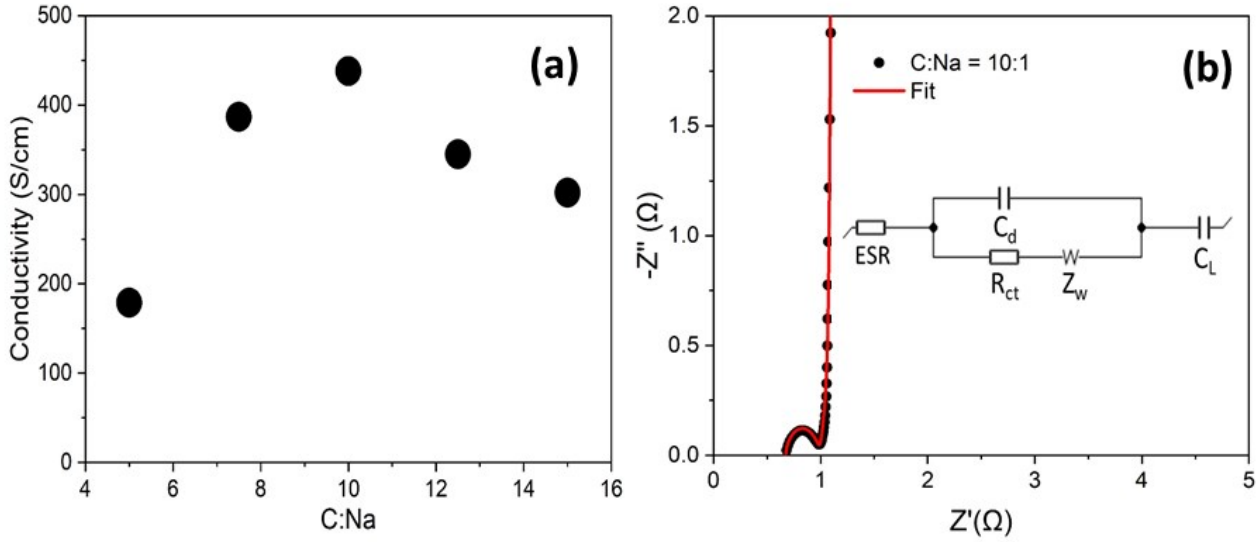

Fig. S4 (a) Electrical conductivity of nanotubide buckypapers at different C:Na but constant absolute nanotubide concentration (1.5 mg/ml). (b) Fitted Nyquist plot of optimized nanotubide buckypaper electrode with inset diagram of equivalent circuit.

Table S1. Charge transfer resistance (R_{ct}) of nanotubide buckypaper at different C:Na obtained by simulating the equivalent circuit.[3, 4]

C:Na	Rct (Ω)
5:1	0.55
7.5:1	0.27
10:1	0.32
12.5:1	0.1
15:1	0.05

Table S2. Element composition in buckypapers, determined by XPS

Sample	XPS		
	at% C	at% O	at% Fe
Sonicated SWCNT buckypaper	94.23	5.46	0.31
Nanotubide buckypaper ([C] = 1.5 mg/ml,C:Na =10:1).	95.09	4.74	0.17

Table S3. Gravimetric and volumetric capacitance of carbon-based buckypaper electrodes, compared to those reported in the literature.

Note: All volumetric capacitances are calculated from total volume of electrode active materials**.**

Electrode materials	C_s (F/g)	C_v (F/cm^3)	Electrolyte	Ref.
GO/FWNT	-	39 (50 mA/cm^3)	1M H_2SO_4	[5]
Cross-linked graphene aerogel (compressed)	130 (10 mV/s)	14 (10 mV/s)	1 M H_2SO_4	[6]
Graphene/CNT aerogel (compressed)	40 (1 A/g)	5 (1 A/g)	1 M Na_2SO_4	[7]
Reduced graphene (MPG)	-	18	H_2SO_4/PVA	[8]
RGO-SO_3H-MWCNT(25%)	53 (2 m V/s)	58 (2 m V/s)	H_2SO_4/PVA	[9]
rGO/poly(vinyl pyrrolidone) (PVP)	168 (1 A/g)	67 (1 A/g)	H_3PO_4/PVA	[10]
Holey graphene film	45 (3 A/g)	54 (3 A/g)	EMITFSI	[11]
MWCNT buckypaper	180 (10 mV/s) 85 (100 mV/s)	75 (10 mV/s) 37 (100 mV/s)	1M Na_2SO_4	[12]
V-Aligned SWCNT buckypaper	80	45.6	Et_4NBF_4/propylene carbonate	[13]
Sonicated SWCNT buckypaper	**82 (10 mV/s)** **41 (100 mV/s)**	**10 (10 mV/s)** **5 (100 mV/s)**	**1M H_2SO_4**	**This work**
Nanotubide buckypaper	**218 (10 mV/s)** **172 (100 mV/s)**	**74 (10 mV/s)** **58 (100 mV/s)**	**1M H_2SO_4**	**This work**

3. Symmetric supercapacitors implementing nanotubide buckypaper electrodes

3.1 Comparison of BC nanopaper and cellulose paper as separators in 1 M H_2SO_4.

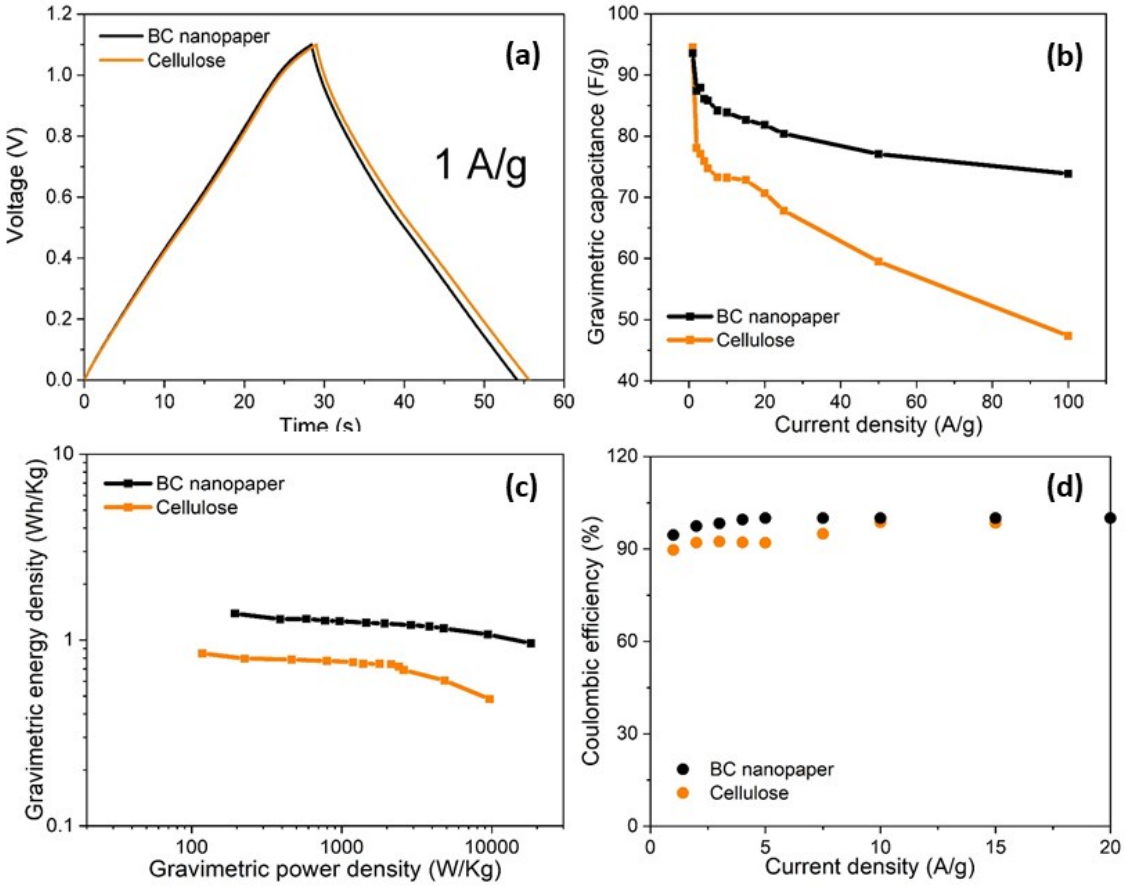

Fig.S5 Nanotubide buckypaper symmetric supercapacitors using BC nanopaper (black) and cellulose (orange) as a separator with 1 M H_2SO_4: (a) GCD curves at 1A/g and (b) the calculated gravimetric capacitance at current density from 1 to 100 A/g normalised by mass of active materials and multiplied by 4 in order to compare the capacitance with 3-electrode system, (c) gravimetric Ragone plots normalised by total mass of device and (d) Coulombic efficiency vs. current density.

3.2 Symmetric supercapacitor of nanotubide buckypaper using BC nanopaper separator with [EMIM][TFSI] ionic liquid electrolyte.

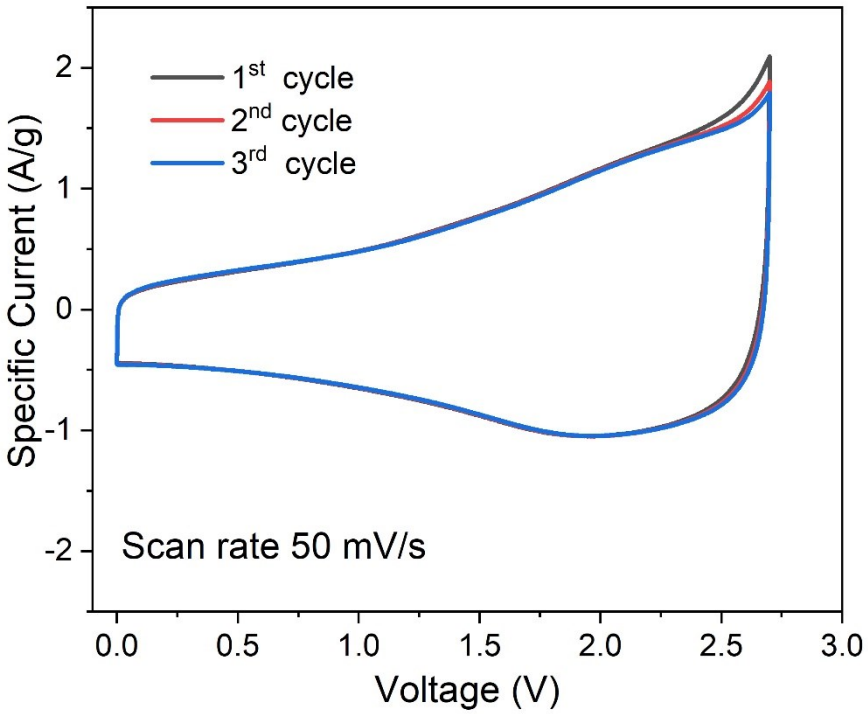

Fig.S6 CV curves at 50 mV/s of nanotubide buckypaper symmetric full cell supercapacitor using BC nanopaper as a separator with [EMIM][TFSI] ionic liquid electrolyte.

Table S4. The electrochemical performance of CNT based film symmetric supercapacitors normalised by mass and volume of active materials.

CNTs supercapactiors	Electrode Thickness (μm)	m_{area} (mg/cm²)	Electrolyte	Operating voltage (V)	C_s (1) (F/g)	$E_{gravimetric}$ (2) (Wh/kg)	$P_{gravimetric}$ (2) (W/kg)	$E_{volumetric}$ (3) (mWh/cm³)	$P_{volumetric}$ (3) (mW/cm³)	Reference
VF MWCNTs	20	-	1 M H_2SO_4	1 V	39 (1 mA)	0.02	5.8	-	-	[14]
Nitrogen-doped carbon/CNT	36	2.45	H_2SO_4/PVA	1 V	-	1.5	211	0.5	72	[15]
FCCVD SWCNT film	20	0.036	H_2SO_4/PVA	0.8	48 (10 A/g)	0.98	960	0.01	8.64	[16]
Buckled SWNT	5	0.009	Ionic liquid ($TEABF_4$/PC)	1.5 V	54 (1 A/g)	3.8	330	0.91	79	[17]
SWCNT macrofilm	-	0.24	Ionic liquid ($TEABF_4$/PC)	1.5 V	44 (10 A/g)	3.24	1560	-	-	[18]
Nanotubide buckypaper	38	**1.3**	**1 M H_2SO_4**	**1.1 V**	**80 (10 A/g)**	**3.9**	**550**	**1.4**	**190**	**This work**
Nanotubide buckypaper	38	**1.3**	**Ionic liquid ([EMIM][TFSI])**	**2.7 V**	**23 (10 A/g)**	**8.8**	**1585**	**2.3**	**420**	**This work**

Note: The positive and negative electrodes thickness are approximately equal and m_{area} is total mass of positive and negative electrodes devided by total area of positive and negative electrodes

(1) Specific capacitance of active materials calculated by equation S8

(2) Gravimetric energy and power density per unit weight of active materials

(3) Volumetric energy and power density per unit volume of active materials

References

1. Y. J. Lee, S. R. Ham, J. H. Kim, T. H. Yoo, S. R. Kim, Y. T. Lee, D. K. Hwang, B. Angadi, W. S. Seo, B. K. Ju and W. K. Choi, *Scientific Reports*, 2018, **8**, 4851.
2. Z. R. Yue, W. Jiang, L. Wang, S. D. Gardner and C. U. Pittman, *Carbon*, 1999, **37**, 1785-1796.
3. Q. Liu, Q. Shi, H. Wang, Q. Zhang and Y. Li, *RSC Advances*, 2015, **5**, 47074-47079.
4. M. Deraman, N. S. M. Nor, N. H. Basri, B. N. M. Dollah, S. Soltaninejad, R. Daik, R. Omar, M. A. Hashim@Ismail and M. A. R. Othman, *Advanced Materials Research*, 2015, **1112**, 231-235.
5. Y. Ma, P. Li, J. W. Sedloff, X. Zhang, H. Zhang and J. Liu, *ACS Nano*, 2015, **9**, 1352-1359.
6. J.-Y. Hong, B. M. Bak, J. J. Wie, J. Kong and H. S. Park, *Advanced Functional Materials*, 2015, **25**, 1053-1062.
7. E. Wilson and M. F. Islam, *ACS Applied Materials & Interfaces*, 2015, **7**, 5612-5618.
8. Z. S. Wu, K. Parvez, X. Feng and K. Müllen, *Nature Communications*, 2013, **4**, 2487.
9. H. Yoo, M. Min, S. Bak, Y. Yoon and H. Lee, *Journal of Materials Chemistry A*, 2014, **2**, 6663-6668.
10. L. Huang, C. Li and G. Shi, *Journal of Materials Chemistry A*, 2014, **2**, 968-974.
11. X. Han, M. R. Funk, F. Shen, Y.-C. Chen, Y. Li, C. J. Campbell, J. Dai, X. Yang, J.-W. Kim, Y. Liao, J. W. Connell, V. Barone, Z. Chen, Y. Lin and L. Hu, *ACS Nano*, 2014, **8**, 8255-8265.
12. B. Pandit, S. R. Dhakate, B. P. Singh and B. R. Sankapal, *Electrochimica Acta*, 2017, **249**, 395-403.
13. D. N. Futaba, K. Hata, T. Yamada, T. Hiraoka, Y. Hayamizu, Y. Kakudate, O. Tanaike, H. Hatori, M. Yumura and S. Iijima, *Nature Materials*, 2006, **5**, 987-994.
14. M. Kaempgen, J. Ma, G. Gruner, G. Wee and S. G. Mhaisalkar, *Applied Physics Letters*, 2007, **90**, 264104.
15. D. K. Kim, N. D. Kim, S.-K. Park, K.-d. Seong, M. Hwang, N.-H. You and Y. Piao, *Journal of Power Sources*, 2018, **380**, 55-63.
16. Z. Niu, H. Dong, B. Zhu, J. Li, H. H. Hng, W. Zhou, X. Chen and S. Xie, *Advanced Materials*, 2013, **25**, 1058-1064.
17. C. Yu, C. Masarapu, J. Rong, B. Wei and H. Jiang, *Advanced Materials*, 2009, **21**, 4793-4797.
18. X. Li, T. Gu and B. Wei, *Nano Letters*, 2012, **12**, 6366-6371.